Chemical Science

ROYAL SOCIETY OF CHEMISTRY

EDGE ARTICLE

Cite this: *Chem. Sci.*, 2021, **12**, 8199

All publication charges for this article have been paid for by the Royal Society of Chemistry

Photo-induced ultralong phosphorescence of carbon dots for thermally sensitive dynamic patterning†

Yanfeng Liu,‡[ac] Xin Huang,‡[a] Zuoji Niu,‡[b] Dongni Wang,[a] Huilin Gou,[a] Qiaobo Liao,[a] Kai Xi,*[a] Zhongfu An*[b] and Xudong Jia*[ac]

Stimuli-responsive films with a dynamic long afterglow feature have received considerable attention in the field of optical materials. Herein, we report the unique dynamic ultralong room temperature phosphorescence (URTP) in flexible solid films made of luminescent carbon dots (CDs) and polyvinylpyrrolidone (PVP). Impressively, fully reversible photo-activation and thermal deactivation of the dynamic long afterglow was achieved in this material, with a lifetime on–off ratio exceeding 3900. Subsequently, ultra-fine URTP patterns (resolution > 1280 dpi) with thermally sensitive retention time were readily photo-printed onto the films and utilized as time–temperature indicating logistics labels with multi-editing capacity. These findings not only enrich the library of dynamic URTP materials, but also extend the scope of the potential applications of luminescent CDs.

Received 10th March 2021
Accepted 8th May 2021

DOI: 10.1039/d1sc01394g

rsc.li/chemical-science

Introduction

Ultralong room temperature phosphorescent (URTP) materials with luminescence lifetime exceeding 100 ms have garnered intense research interest in recent years.[1–19] The long afterglow emission (lasting for seconds to hours after excitation) of these materials provides time-resolved optical information with an outstanding signal-to-noise ratio, which endorses their vast applications in different fields including optical encryption and anti-counterfeiting,[1–3,12–15,17–19] illumination/display,[9] bio-imaging,[4,11] *etc.* Compared to their inorganic counterparts, organic URTP materials like molecular crystals or amorphous polymer composites show significant advantages such as lower cost, better processability and environmental friendliness. Importantly, organic URTP materials, especially the amorphous ones, are more sensitive to external stimuli,[8,12] and therefore have tremendous potential for the fabrication of smart materials with responsive properties.

Recently, organic materials with dynamic URTP have emerged as a new star of the family.[14–19] Unlike conventional materials that only respond instantly, dynamic URTP materials show switchable optical performance with a significant memory effect after being exposed to stimuli. For example, dynamic URTP with a memory effect has been realized with molecular phosphors that alter between different bistable molecular packing forms upon exposure to photo/thermal stimuli.[14–16] More recently, Gmelch *et al.* developed amorphous polymer coatings with an optically programmable long afterglow.[18,19] These successful examples have brought revolutionary improvements to the performance of organic URTP materials, opening up new fields of applications such as multi-level anti-counterfeiting and dynamic patterning. However, despite the great demand for smart materials with a dynamic long afterglow, their rational design and fabrication remain a daunting challenge.

Fortunately, new opportunities in materials design are being created by carbon dots (CDs). These emerging luminescent nano-dots are small-sized (<10 nm), mass-producible, compatible with organic materials and optically robust.[20–23] Furthermore, the incorporation of CDs with polymers has produced a series of composite films with reliable URTP long afterglow performance,[24–29] enriching the library of transparent and flexible URTP materials. It was recently reported that CDs in polymer matrices can serve not only as URTP emitters, but also as reactive centers that alter the regional environments in the materials, facilitating dynamic URTP performance. For instance, Qu's group successfully triggered URTP enhancement in a composite film by intensifying the crosslinking between CDs and polyvinyl alcohol (PVA) through thermal treatment.[28] Furthermore, Bao *et al.* utilized the photothermal effect of CDs and realized direct photo-writing of URTP patterns on CD/PVA

[a]*School of Chemistry and Chemical Engineering, Nanjing University, 163 Xianlin Road, Nanjing, 210023, China. E-mail: xikai@nju.edu.cn; jiaxd@nju.edu.cn*

[b]*Key Laboratory of Flexible Electronics (KLOFE), Institute of Advanced Materials (IAM), Nanjing Tech University (Nanjing Tech), 30 South Puzhu Road, Nanjing, 211816, China. E-mail: iamzfan@njtech.edu.cn*

[c]*State Key Laboratory of Coordination Chemistry, Nanjing National Laboratory of Microstructures, Nanjing University, 163 Xianlin Road, Nanjing, 210023, China. E-mail: jiaxd@nju.edu.cn*

† Electronic supplementary information (ESI) available. See DOI: 10.1039/d1sc01394g

‡ These three authors contributed equally to the work.

films with a near-infrared laser.[29] However, CD-based dynamic URTP materials still suffered from harsh working conditions, slow response, irreversibility and insufficient spatial accuracy, which altogether hampered their practical application in programmable optical devices.

To this end, we herein propose the design of a flexible CD/polymer composite film showing spatially accurate photo-induced dynamic URTP with a fully reversible memory effect. To realize such advanced performance, triplet oxygen, a well-known quencher of triplet excitons, is intentionally introduced to mediate the dynamic URTP emission. Upon photo-irradiation, CDs embedded in the oxygen-permeable polyvinylpyrrolidone (PVP) matrix continuously generate triplet excitons that remove the triplet oxygen through an *in situ* photodynamic process (I and II in Fig. 1A). After that, the irradiated region gradually becomes anoxic and results in spatially accurate photo-activation of the URTP (III in Fig. 1A). The photo-induced long afterglow memory remains in the pre-irradiated region for a considerable duration, before environmental oxygen permeates the film again, deactivating the URTP. Notably, the oxygen permeability can be tuned through thermal treatment, resulting in thermally sensitive retention time of the memory (IV in Fig. 1A). Utilizing these properties, reversible photo-writing and thermal-erasing of URTP patterns are successfully demonstrated in CD/PVP films. Moreover, editable logistics labels with time–temperature indicating (TTI) functions were realized by virtue of the thermally sensitive URTP of CDs. To the best of our knowledge, this is the first example of a CD-based dynamic URTP material with practical performance.

Experimental

Materials

Reagent grade *p*-benzoquinone (PBQ, CP) and ethylenediamine (EDA, AR) were purchased from Sinopharm Chemical Reagent Co., Ltd. (Shanghai, China). Methanol (AR), ethanol (AR) and dichloromethane (DCM, AR) were purchased from General Reagent, Shanghai Titan Scientific Co., Ltd (Shanghai, China). Polyvinylpyrrolidones (PVPs, average molecular weight: 8 kD/58 kD/360 kD/1300 kD) were purchased from Energy Chemical-Saan Chemical Technology Co., Ltd. (Shanghai, China). Polyacrylamide (PAM, non-ionic, average molecular weight: 150 kD) was purchased from Sigma-Aldrich Co., Ltd. (Shanghai, China). Deionized water was used throughout the study.

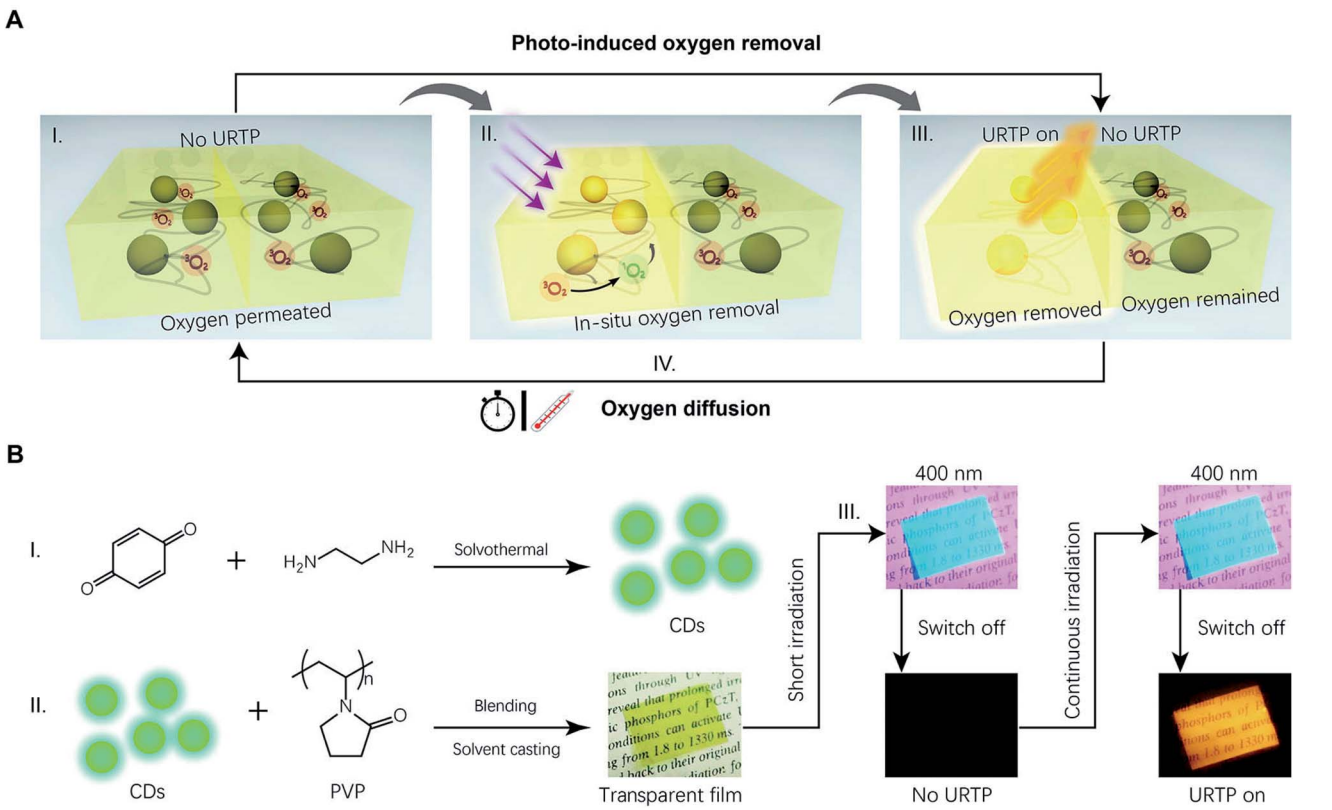

Fig. 1 Schematic illustration for the design and fabrication of the CD/PVP composite film with reversible photo-induced URTP. (A) Diagram of the processes to achieve a dynamic URTP long afterglow. The CD/PVP composite film initially showed no afterglow due to oxygen quenching (I). Upon irradiation, the permeated triplet oxygen was gradually converted to singlet oxygen through a photodynamic process (II), eventually creating a hypoxic area in the exposed region that showed a URTP long afterglow (III). Afterward, the localized hypoxia would last for a certain duration before oxygen replenishment through diffusion (IV), which could be accelerated by thermal treatment. (B) The preparation of the CD/PVP composite film and demonstration of its dynamic URTP. The CDs synthesized from molecular precursors through a solvothermal method (I) were blended with PVP in an aqueous solution and cast into a transparent, flexible film (II). The as-prepared film initially showed no afterglow after short irradiation (400 nm, 10 mW cm^{-2}, <0.5 s); however, an intense long afterglow occurred after prolonged irradiation (30 s).

Characterization

The transmission electron microscopy (TEM) images were acquired using a JEM 2100 instrument (JEOL) (acceleration voltage: 200 kV); the UV-vis absorption spectra were obtained with a UV-3600 spectrophotometer (Shimadzu, Japan); the Fourier transform infrared (FT-IR) absorption spectra were obtained with a NICOLET iS10 FT-IR spectrometer (Thermo Scientific™, America); the X-ray photoelectron spectroscopy (XPS) data, including binding energy survey and high resolution spectra of C 1s, N 1s and O 1s, were acquired on a PHI 5000 Versa Probe (UlVAC-PHI, Japan). The photoluminescence (PL) emission spectra, emission mapping and the photoluminescence quantum yield (PLQY) of CDs in ethanol solution were measured with a FluoroLog FL3 spectrophotometer (HORIBA, Japan). The PL lifetime, URTP lifetime and URTP emission spectra were measured on an FLS980 spectrophotometer (Edinburgh Instrument, UK) equipped with a microsecond flash-lamp (μF900); all URTP emission spectra were measured with the following configuration unless otherwise specified: lamp frequency: 50 Hz, initial delay: 5 ms, sampling window: 15 ms.

Synthesis of CDs

Briefly, 648 mg (6 mmol) of PBQ was dissolved in 200 mL of ethanol under agitation to form a homogeneous solution. To that solution was added 480 mg (8 mmol) of EDA in one portion to form a hazel dispersion, which was further sealed in an autoclave and maintained at 120 °C for 10 h. Afterward, the reaction was naturally cooled down to room temperature. The crude product was collected and concentrated by rotary evaporation under reduced pressure before being further purified by dialysis (cutoff M_w: 5000 D; the crude product was dialyzed against DI water for 48 h with water renewed every 12 h) and silica column chromatography (eluent: 90% dichloromethane and 10% methanol). As a result, about 200 mg of brown powdery product was finally obtained.

Preparation of the CD/PVP composite film

To prepare a CD/PVP composite film, 1 g of PVP was fully dissolved in 19 mL of deionized water under agitation at 328 K (55 °C). Next, 1 mL of ethanol solution containing 5 mg CDs was added to the PVP aqueous solution quickly. The solution was further magnetically stirred for 30 min to ensure a homogeneous dispersion.

Afterward, onto a standard 9 cm × 9 cm square polystyrene Petri dish was poured 17.5 g of the CD/PVP solution. Transferred to a flat heater previously adjusted to 313 K (40 °C), the solution was left for solvent evaporation for 10 h. The resultant film was then heated at 393 K (120 °C) under reduced pressure (~0.1 mbar) for another 2 h for complete drying. The thickness of the as-prepared film was 80 μm (measured with a micrometer screw gauge). Commercially available PET lamination films (purchased from Jiwen Lamination Film Co. Ltd., Wuxi, China) with different thicknesses (50, 80, 100, 125, and 150 μm) were applied to protect the films from being scratched and to adjust their oxygen permeability. In this work, the typical photophysics properties of the material were measured from a sample coated with 80 μm-thick PET, unless otherwise specified.

Results and discussion

To begin with, CDs containing abundant heteroatoms (N and O) were synthesized through a solvothermal method (I in Fig. 1B). In this design, N,O-containing functional groups benefited the URTP of CDs in two major ways. Firstly, N and O atoms contain lone-pair electrons that could facilitate n–π* transitions and enhance the intersystem crossing (ISC),[30,31] promoting the generation of triplet excitons. Secondly, these functional groups could serve as "anchoring spots" for hydrogen bond fixation, which efficiently reduced non-radiative energy loss.[25,26,32] As was validated by structural analysis (Fig. S1–S3, Table S1†), the as-prepared CDs were nano-sized and highly functionalized with amine, imine, hydroxyl, carbonyl and enamine groups, in agreement with our design. At this point, the CDs showed only short-lived fluorescence with a lifetime of 3.3 ns in solution (Fig. S4†); meanwhile in the powdery state, there was no visualized PL emission whatsoever. In contrast, photo-induced URTP occurred in a transparent CD/PVP composite film prepared by solvent-casting (II in Fig. 1B). In this specific composite, PVP acts as a hydrogen-bonded matrix with abundant lactam groups which provide solid fixation that suppresses the non-radiative energy loss and benefits the URTP emission of CDs. Importantly, as a bio-compatible hydrophilic polymer, PVP features excellent oxygen permeability,[33] which fundamentally enables the design of dynamic URTP. Furthermore, PVP is reductive and capable of scavenging the generated singlet oxygen,[34] thereby enabling rapid removal of molecular oxygen and a fast response rate.

The resultant CD/PVP composite film initially emitted bright cyan light upon 400 nm excitation, which instantly disappeared as the irradiation switched off. As expected, the first short irradiation (<0.5 s) did not evoke any observable URTP emission. Impressively, an orange long afterglow occurred after the film was continuously irradiated with a 400 nm UV lamp (III in Fig. 1B and 2A). The photo-activation of dynamic URTP significantly prolonged the luminescence lifetime of the material by 3932 times (from 148 μs to 582 ms; Fig. 2B and Table S2†). The fully activated URTP caused by the regional photo-induced hypoxia naturally lasted for more than 1 h at room temperature, before it gradually disappeared due to oxygen permeation. In addition, the photo-induced URTP could be quickly executed within minutes by thermal treatment. Such an on–off switch could be repeated for multiple cycles without causing significant deterioration of the long afterglow performance (Fig. 2C and S5†).

In a further set of experiments, the response of the photo-induced URTP under different conditions was studied. From Fig. 2D, it was found that the time required to turn on the afterglow clearly decreased with increasing irradiation power density. Specifically, the time required to achieve half-maximal URTP intensity ($t_{1/2}$) was inversely proportional to the irradiation power density (Fig. S6†). Estimating from that, with an

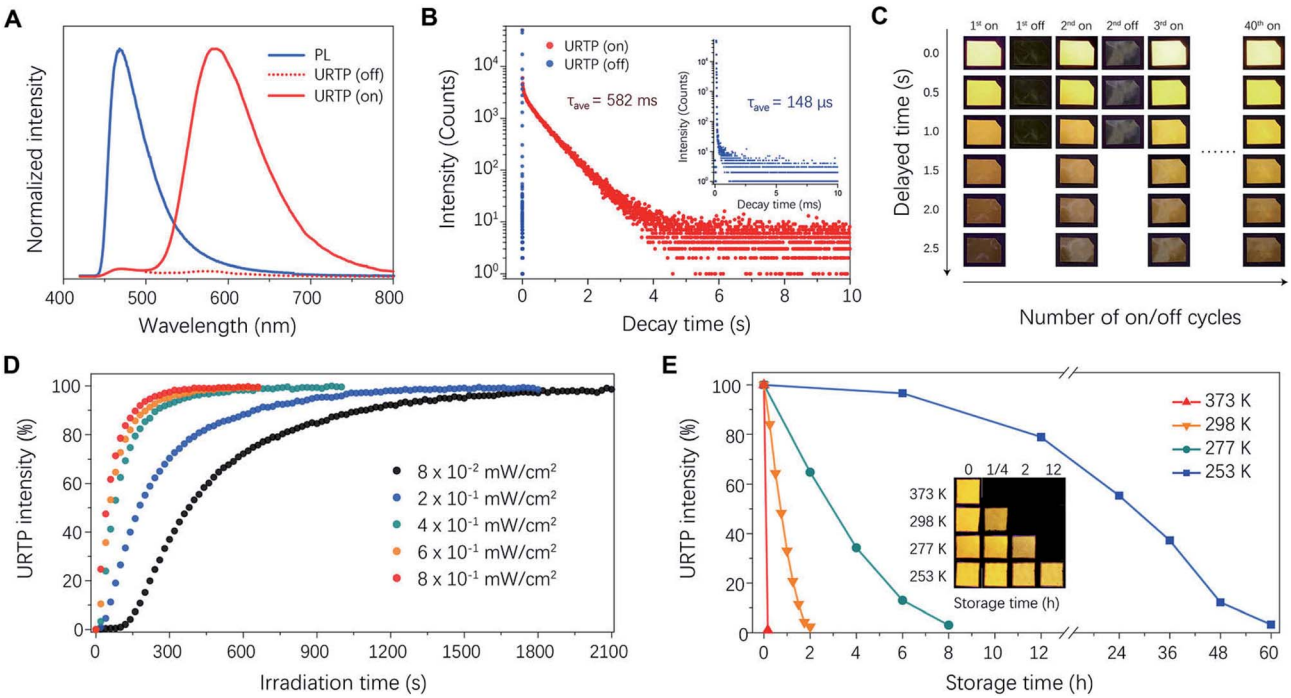

Fig. 2 Photophysical properties of the CD/PVP film. (A) The steady-state PL emission (solid blue line) and URTP spectra (dotted and solid red lines) of a CD/PVP composite film. The PL emission of the film peaked at 470 nm, slightly blue-shifted compared with solution phase emission (Fig. S4†). The URTP emission intensity of the composite was initially low (dotted red line), and then it significantly increased after the composite was continuously irradiated with a 400 nm flashlight for 30 s (solid red line). The fully activated URTP peaked at 580 nm. (B) The PL decay profile of the film before (blue dots) and after (red dots) photo-activation. (C) Photographs of the film with and without the long afterglow feature at different on–off switch cycles. (D) URTP intensity plotted against irradiation time under different power densities. (E) URTP intensity plotted against storage time at different temperatures (inset: photographs of the film's long afterglow examined after gradually extending storage time at different temperatures).

irradiation power density of 10 mW cm^{-2}, the URTP intensity would reach 50% maximum within 4 s and 90% maximum within 20 s under continuous irradiation, allowing the rapid recording of optical information. Meanwhile, the decreasing rate of the dynamic URTP was evidently thermally sensitive due to the enhancement of oxygen permeation under higher temperature. For instance, the memory of URTP quickly vanished at 373 K within 15 min, but remained detectable at 253 K even after 48 h (Fig. 2E). Such character indicated that CD/PVP could serve as a temporal memory medium that preserves URTP under ambient or lower temperature, and quickly erases it when exposed to heat. Additionally, we also found that the retention time of dynamic URTP could be further tuned by adjusting the molecular weight of PVP, or simply applying surface barrier layers with different thicknesses (Fig. S7†). The influence of moisture on the URTP performance was also studied. As shown in Fig. S8,† the fully activated URTP intensity of the CD/PVP film evidently decreased with increasing moisture content due to interference from hydrogen fixation, but fully recovered after the material was thermally dried.

To further validate the essential character of oxygen in the dynamic URTP long afterglow, a different composite film was prepared using CDs blended with polyacrylamide (PAM) instead of PVP, and studied as a control group. Different from the oxygen-permeable PVP, PAM features minimal oxygen permeability,[35] which leads to a constant anoxic environment in the composite film. The emission wavelength and decay profiles of the CD/PAM composite are similar to those of photo-activated CD/PVP composites (Fig. S9 and Table S3†).The comparison of a pure PAM film and the CD/PAM composite further confirmed that the orange long afterglow originated from the phosphorescent emission of CDs (Fig. S10†). The difference occurred, however, when the URTP emissions of two different composite films were examined under intermittent irradiation with a regular "on–off" switching pattern (Fig. 3A). In this case, the CD/PVP composite film showed a gradually accumulating URTP intensity with an evident memory effect, while the CD/PAM composite film showed a constant URTP intensity that almost instantly reached its maximum as the irradiation switched on. A more straight-forward demonstration is shown in Fig. 3B and Video S1,† where the CD/PAM composite showed an intrinsic URTP nature, but CD/PVP clearly showed spatially accurate dynamic URTP and only emitted a long afterglow in the photo-activated region. The above-mentioned results validated that adequate oxygen permeability of the material was crucial to achieving the unique dynamic URTP. The oxygen-mediated photo-activation mechanism was further validated by the following experiments. Firstly, the URTP emission of CD/PVP films was measured under aerated and degassed conditions (Fig. S11†). As a result,

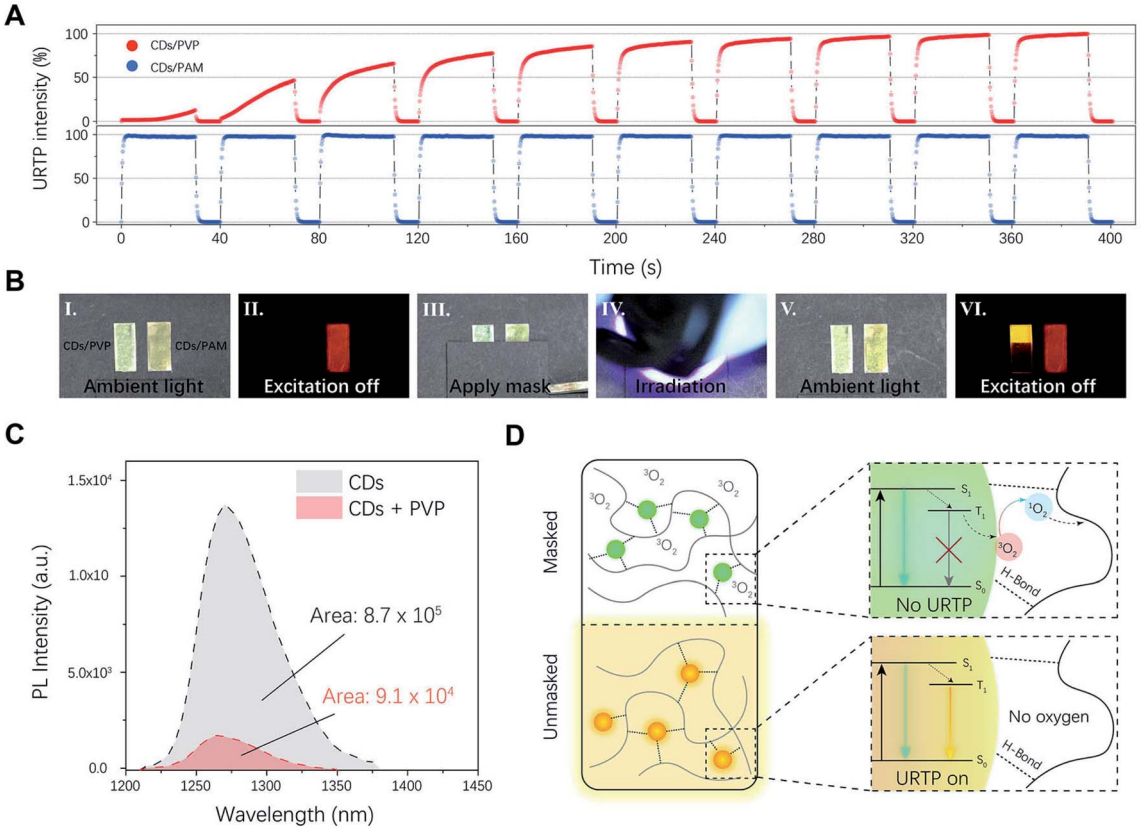

Fig. 3 Mechanistic investigation of the oxygen mediated photo-induced URTP. (A) The normalized URTP intensity of CD/PVP and CD/PAM films against time upon intermittent irradiation (0.8 mW cm^{-2}, 30 s irradiation followed by 10 s darkness) cycles. The URTP intensity of CD/PVP clearly showed gradual accumulation, while the URTP intensity of CD/PAM is almost constant in each irradiation window. (B) Photographs of CD/PVP (①) and CD/PAM (②) films upon photo-activation and excitation. The two films were placed side by side for demonstration (I). After short irradiation with a 400 nm lamp, only ② showed an observable afterglow (II). A mask was applied to cover the lower half of both films (III) before performing continuous irradiation (IV). Afterward, the mask was removed, and no significant morphological change occurred when inspected under ambient light (V). Another short irradiation revealed the change of URTP memory in film ① after continuous irradiation (VI). (C) The NIR luminescence of singlet oxygen in D_2O solutions containing only CDs (0.25 wt‰) and CDs + PVP (CDs: 0.25 wt‰, PVP: 5 wt%) under continuous 400 nm irradiation. (D) Schematic illustration of the oxygen-mediated dynamic URTP in masked and unmasked regions under excitation.

the fully degassed film showed a constant long afterglow, while the aerated film only showed delayed emission after photo-activation, suggesting that the triplet oxygen in the aerated film is responsible for the suppression of its phosphorescent emission. Secondly, the near-infrared (NIR) luminescence of singlet oxygen[36] in the CD solution was measured under UV irradiation. As shown in Fig. 3C, evident NIR emission was detected from the CD solution under 400 nm irradiation, suggesting that triplet oxygen molecules were converted into singlet oxygen through a photodynamic process. The NIR emission intensity dramatically decreased in the presence of PVP, indicating the consumption of the singlet oxygen by the reductive macromolecules (Fig. 3D).

Notably, excitation light activates the dynamic URTP with high spatial accuracy, which allows ink-free printing of optical patterns with masking and lithography methods. The limiting line resolution of such patterns was up to 20 μm when examined with a standard USAF-1951 target (Fig. S12†), which equaled ~1280 dpi. By combining the photo-activation and thermal deactivation of dynamic URTP, reversible writing–reading–erasing cycles of different long afterglow patterns could be readily achieved (Fig. 4A, Video S2†). It's worth mentioning that the write-in and read-out of dynamic URTP could also be accomplished with a commercial white light LED lamp (Video S3†), which further added to the applicability of this material. During this process, the transmittance, morphology, and steady-state PL emission of the film remained almost unchanged (see Fig. S13 and S14†), which altogether made this material naturally suitable for practical applications like graphic encryption or anti-counterfeiting (see Fig. S15†).

Given the spatial accuracy of the photo-activation and temperature dependency of the thermal deactivation, we further envision the potential application of this dynamic URTP composite as a multi-editable logistics label with time–temperature indicating functions for cold-chain. The delivery of many medicines or vaccines relies on cold-chain transportation, where they are constantly maintained at low temperature to prevent thermally induced deterioration. The failure of cold-chain or temperature abuse causes not only financial loss, but also a potential public hygiene hazard.[37] Such issues have only

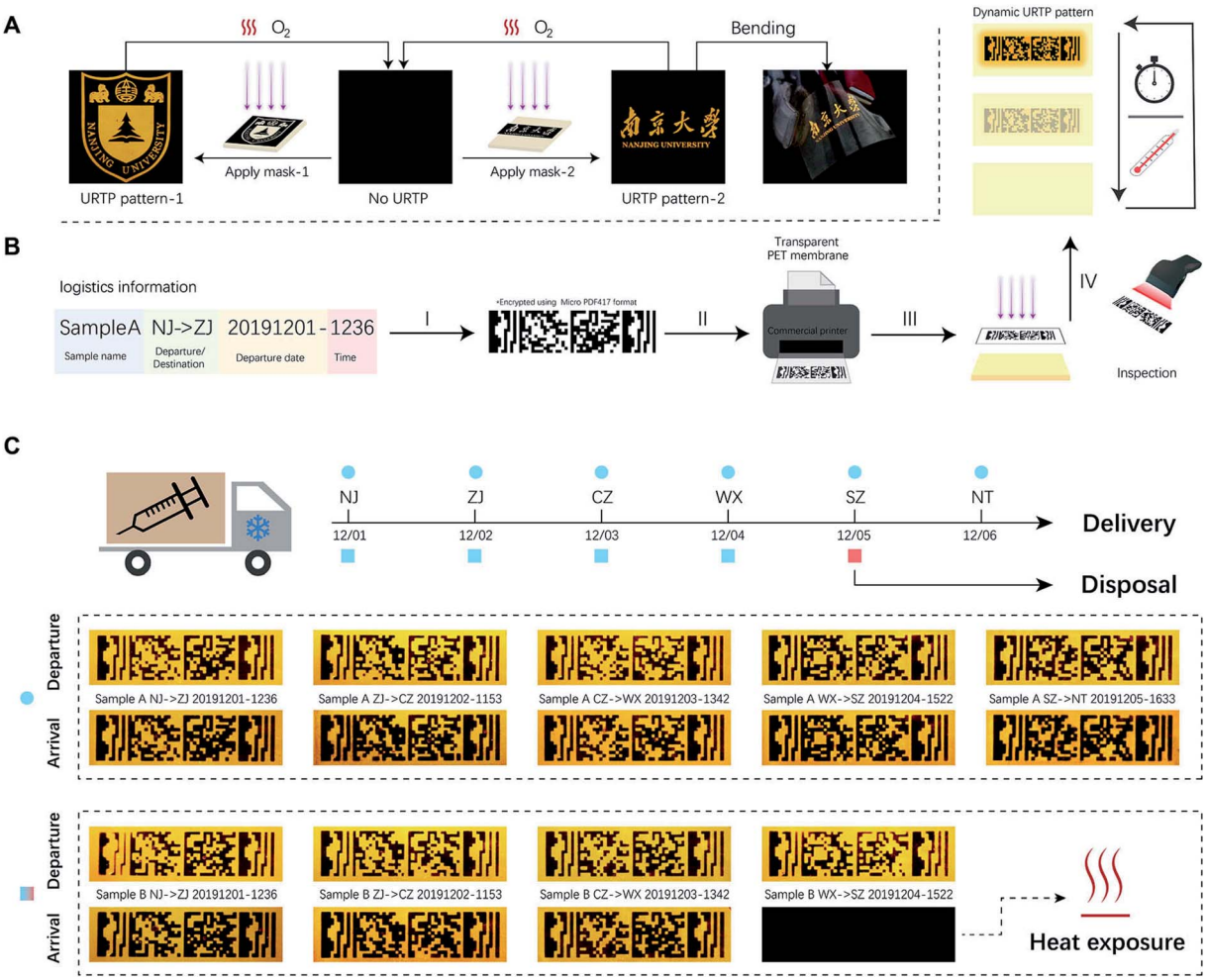

Fig. 4 Reversible URTP photo-patterning of CD/PVP films and their application as time–temperature indicating logistics labels. (A) Illustration of the ink-free optical printing of dynamic URTP patterns by masking and lithography. Emblem and Chinese characters (URTP pattern-1 and pattern-2) were created with different masks successively on the same film after the previous pattern was erased by thermal treatment. Bending the flexible film did not affect the display quality. (B) Schematic illustration of the use of editable CD/PVP labels with thermally sensitive dynamic URTP memory. Firstly, the logistics data were filed and encrypted into a 2D barcode using the Micro-PDF417 format (I). Then, the barcode was printed onto a transparent PET membrane using a commercial static printer to obtain a print-on-demand mask (II). By applying that mask for photolithography (III), a long afterglow pattern containing logistics data was created on the tag (IV). The edited labels were then packaged with the cargo, being regularly inspected, erased, and updated at each stop during the delivery. (C) Flowchart: a hypothetical multi-drop cold-chain transportation route through which thermally sensitive cargo (samples A and B were denoted by dots and squares, respectively) were delivered. Photographs: dynamic URTP patterns on labels referring to sample A (top) and sample B (bottom) upon departure and arrival at each stage.

become more urgent during the Covid-19 crisis, as many of the currently developed vaccines require storage below freezing point.[38] TTI devices like WarmMark (SpotSee™) are powerful tools to indicate and prevent cold-chain failure. Typically, these tags could indicate the cumulative effect of heat exposure by altering their optical appearance (for example, through the change of color or graphic pattern). However, most of the commercially available TTI tags are intended for single use only and lack editability, which might make them incompetent for the global delivery of vaccines with large cargo traffic volume and multi-drop routes. In this sense, the development of multi-use smart labels combining editable logistics information and time-temperature indicating functions would be desirable.

To this end, we proposed to utilize the CD/PVP composite films as editable smart logistics labels with TTI functions (Fig. 4B). Herein, we conceived a hypothetical 6-step transportation route to demonstrate the application of the editable logistics-TTI labels. As was demonstrated in Fig. 4C, two tags labeled as sample A and sample B were used to demonstrate the cases of successful maintenance and segmental failure of the cold-chain, respectively.

During the transportation, logistics information was optically printed upon departure and inspected upon arrival at each segment. The URTP photographs of the two labels upon departure and arrival were captured and are listed in Fig. 4C. In the first three transport segments (NJ → JZ, JZ → CZ, and CZ → WX), both labels were well-preserved at 253 K. At this stage, all

graphic information could be readily recognized upon arrival. At the fourth segment between WX and SZ, while sample A was constantly kept at 253 K, sample B was exposed to room temperature (298 K) for 1 h during this process. As a result, upon arrival at SZ, only the sample A tag retained a recognizable barcode pattern. Meanwhile, no information could be read from the sample B tag after multiple attempts (Fig. S16 and Video S4†), which indicated the potential deterioration of the cargo.

Conclusions

In summary, we presented a rational design of flexible composite films with reversible dynamic URTP, based on the combination of the CD phosphor and an oxygen-permeable polymer, PVP. The photo-activation of URTP in CD/PVP films was efficient and accurate, which supported their application in temporary optical patterning. Meanwhile, the thermal-deactivation rate of URTP in CD/PVP is highly dependent on temperature, thus enabling time–temperature indicating functions. On this basis, the potential applications of this material as multi-editable optical labels with time-temperature indicating functions for cold-chain logistics were demonstrated. Our findings in this work not only open up a new field of CD-based smart optical materials, but also provide novel ideas for the production of flexible stimuli-responsive materials with a URTP long afterglow.

Author contributions

Y. L., K. X., Z. A. and X. J. initiated, managed and planned the overall project. Y. L., X. H. and Z. N. were primarily responsible for the experiments. Y. L. and X. H. prepared and characterized the carbon dots and the composite materials. Y. L. and Z. N. measured the photophysical properties of the materials. Y. L. conceived and performed the applications of the material. Y. L., K. X., Z. A. and X. J. prepared the paper. All authors contributed to data analysis, and manuscript refinement and preparation.

Conflicts of interest

There are no conflicts to declare.

Acknowledgements

We thank Professor Fei Xu and PhD candidate Yifeng Xiong for technical assistance. This work is supported by the National Key R&D Program of China (No. 2017YFA0700503), the Fundamental Research Funds for the Central Universities (No. 14380221) and the National Natural Science Foundation of China (No. 21875102, 21875104)

Notes and references

1 Z. An, C. Zheng, Y. Tao, R. Chen, H. Shi, T. Chen, Z. Wang, H. Li, R. Deng, X. Liu and W. Huang, *Nat. Mater.*, 2015, **14**, 685–690.

2 L. Gu, H. Shi, L. Bian, M. Gu, K. Ling, X. Wang, H. Ma, S. Cai, W. Ning, L. Fu, H. Wang, S. Wang, Y. Gao, W. Yao, F. Huo, Y. Tao, Z. An, X. Liu and W. Huang, *Nat. Photonics*, 2019, **13**, 406–411.

3 D. Tu, S. Cai, C. Fernandez, H. Ma, X. Wang, H. Wang, C. Ma, H. Yan, C. Lu and Z. An, *Angew. Chem., Int. Ed.*, 2019, **58**, 9129–9133.

4 X. Zhen, Y. Tao, Z. An, P. Chen, C. Xu, R. Chen, W. Huang and K. Pu, *Adv. Mater.*, 2017, **29**, 1606665.

5 J. Wang, Y. Fang, C. Li, L. Niu, W. Fang, G. Cui and Q. Yang, *Angew. Chem., Int. Ed.*, 2020, **59**, 10032–10036.

6 X. Wang, H. Shi, H. Ma, W. Ye, L. Song, J. Zan, X. Yao, X. Ou, G. Yang, Z. Zhao, M. Singh, C. Lin, H. Wang, W. Jia, Q. Wang, J. Zhi, C. Dong, X. Jiang, Y. Tang, X. Xie, Y. Yang, J. Wang, Q. Chen, Y. Wang, H. Yang, G. Zhang, Z. An, X. Liu and W. Huang, *Nat. Photonics*, 2021, **15**, 187–192.

7 D. Li, F. Lu, J. Wang, W. Hu, X.-M. Cao, X. Ma and H. Tian, *J. Am. Chem. Soc.*, 2018, **140**, 1916–1923.

8 T. Ogoshi, H. Tsuchida, T. Kakuta, T. Yamagishi, A. Taema, T. Ono, M. Sugimoto and M. Mizuno, *Adv. Funct. Mater.*, 2018, **28**, 1707369.

9 S. Kuila, S. Garain, S. Bandi and S. J. George, *Adv. Funct. Mater.*, 2020, **30**, 2003693.

10 Y. Wang, S. Tang, Y. Wen, S. Zheng, B. Yang and W. Z. Yuan, *Mater. Horiz.*, 2020, **7**, 2105–2112.

11 Q. Huang, H. Gao, S. Yang, D. Ding, Z. Lin and Q. Ling, *Nano Res.*, 2020, **13**, 1035–1043.

12 S. Cai, H. Ma, H. Shi, H. Wang, X. Wang, L. Xiao, W. Ye, K. Huang, X. Cao, N. Gan, C. Ma, M. Gu, L. Song, H. Xu, Y. Tao, C. Zhang, W. Yao, Z. An and W. Huang, *Nat. Commun.*, 2019, **10**, 4247.

13 Y. Su, Y. Zhang, Z. Wang, W. Gao, P. Jia, D. Zhang, C. Yang, Y. Li and Y. Zhao, *Angew. Chem., Int. Ed.*, 2020, **59**, 9967–9971.

14 L. Gu, H. Shi, M. Gu, K. Ling, H. Ma, S. Cai, L. Song, C. Ma, H. Li, G. Xing, X. Hang, J. Li, Y. Gao, W. Yao, Z. Shuai, Z. An, X. Liu and W. Huang, *Angew. Chem., Int. Ed.*, 2018, **57**, 8425–8431.

15 J. Yang, X. Zhen, B. Wang, X. Gao, Z. Ren, J. Wang, Y. Xie, J. Li, Q. Peng, K. Pu and Z. Li, *Nat. Commun.*, 2018, **9**, 840.

16 S. Hirata, K. Totani, H. Kaji, M. Vacha, T. Watanabe and C. Adachi, *Adv. Opt. Mater.*, 2013, **1**, 438–442.

17 Y. Su, S. Z. F. Phua, Y. Li, X. Zhou, D. Jana, G. Liu, W. Q. Lim, W. K. Ong, C. Yang and Y. Zhao, *Sci. Adv.*, 2018, **4**, eaas9732.

18 M. Gmelch, H. Thomas, F. Fries and S. Reineke, *Sci. Adv.*, 2019, **5**, eaau7310.

19 H. Thomas, D. L. Pastoetter, M. Gmelch, T. Achenbach, A. Schlögl, M. Louis, X. Feng and S. Reineke, *Adv. Mater.*, 2020, **32**, 2000880.

20 Y. Sun, B. Zhou, Y. Lin, W. Wang, K. A. S. Fernando, P. Pathak, M. J. Meziani, B. A. Harruff, X. Wang, H. Wang, P. Luo, H. Yang, M. E. Kose, B. Chen, L. M. Veca and S. Xie, *J. Am. Chem. Soc.*, 2006, **128**, 7756–7757.

21 Z. Wang, Y. Liu, S. Zhen, X. Li, W. Zhang, X. Sun, B. Xu, X. Wang, Z. Gao and X. Meng, *Adv. Sci.*, 2020, **7**, 1902688.

22 C. Xia, S. Zhu, T. Feng, M. Yang and B. Yang, *Adv. Sci.*, 2019, **6**, 1901316.

23 K. Jiang, X. Gao, X. Feng, Y. Wang, Z. Li and H. Lin, *Angew. Chem., Int. Ed.*, 2020, **59**, 1263–1269.
24 Y. Chen, J. He, C. Hu, H. Zhang, B. Lei and Y. Liu, *J. Mater. Chem. C*, 2017, **5**, 6243–6250.
25 Y. Deng, D. Zhao, X. Chen, F. Wang, H. Song and D. Shen, *Chem. Commun.*, 2013, **49**, 5751.
26 K. Jiang, L. Zhang, J. Lu, C. Xu, C. Cai and H. Lin, *Angew. Chem., Int. Ed.*, 2016, **55**, 7231–7235.
27 J. He, Y. He, Y. Chen, X. Zhang, C. Hu, J. Zhuang, B. Lei and Y. Liu, *Chem. Eng. J.*, 2018, **347**, 505–513.
28 Z. Tian, D. Li, E. V. Ushakova, V. G. Maslov, D. Zhou, P. Jing, D. Shen, S. Qu and A. L. Rogach, *Adv. Sci.*, 2018, **5**, 1800795.
29 X. Bao, E. V. Ushakova, E. Liu, Z. Zhou, D. Li, D. Zhou, S. Qu and A. L. Rogach, *Nanoscale*, 2019, **11**, 14250–14255.
30 R. Article, J. Zhao, W. Wu, J. Sun and S. Guo, *Chem. Soc. Rev.*, 2013, **42**, 5323.
31 Q. Li, Y. Tang, W. Hu and Z. Li, *Small*, 2018, **14**, 1801560.
32 Y. Gao, H. Zhang, Y. Jiao, W. Lu, Y. Liu, H. Han, X. Gong, S. Shuang and C. Dong, *Chem. Mater.*, 2019, **31**, 7979–7986.
33 O. Z. Higa, S. O. Rogero, L. D. D. B. Machado, M. B. Mathor and A. B. Lugão, *Radiat. Phys. Chem.*, 1999, **55**, 705–707.
34 J. Lin, S. Wan, W. Liu and W. Lu, *Chem. Commun.*, 2019, **55**, 4299–4302.
35 W. Jang, I. Rawson and J. C. Grunlan, *Thin Solid Films*, 2008, **516**, 4819–4825.
36 A. U. Khan and M. Kasha, *Proc. Natl. Acad. Sci. U. S. A.*, 1979, **76**, 6047–6049.
37 E. Weir, *Can. Med. Assoc. J.*, 2004, **171**, 1050.
38 D. Pushparajah, S. Jimenez, S. Wong, H. Alattas, N. Nafissi and R. A. Slavcev, *Adv. Drug Delivery Rev.*, 2021, **170**, 113–141.